A CFD SIMULATION ON EFFECTS OF METHANE/BIOGAS RATIO ON 2-STROKE FREE-PISTON LINEAR ENGINE'S SCAVENGING

Ho Van Phuc[1], Nguyen Huynh Thi[2], Huynh Thanh Cong[1], Nguyen Van Trang[2]
[1]*University of Technology, Vietnam National University-Ho Chi Minh City, Vietnam*
[2]*Ho Chi Minh City University of Technology and Education, Vietnam*

Received 28/7/2020, Peer reviewed 3/8/2020, Accepted for publication 4/8/2020.

ABSTRACT

On the work of investigating the effect of methane percentage in biogas on the two-stroke free-piston linear engine (FPLE) power output, a scavenging simulation implementation is required. Although the computational fluid dynamics (CFD) method was recognized as an effective solution, the result may, however, be not precise if the boundary conditions and the gas properties are determined inaccurately. This paper represents a CFD scavenging simulation, in which, a zero-dimensional model for the unsteady flow into the bounce-chamber based on Reynolds transport theorem was built to observe the scavenging's boundary conditions. Simultaneously, the mixture characteristics following methane percentage and temperature are also estimated, in which, 5 circumstances of biogas component: $40\%\ CH_4$, $50\%\ CH_4$, $60\%\ CH_4$, $70\%\ CH_4$, *and* $100\%\ CH_4$ *that will be inputted in CFD modeling afterward. The result shows that although delivered gas mass is enhanced when using low* $\%CH_4$ *biogas, the volumetric efficiency is decreased, particularly from 0.679 to 0.612 when* $\%CH_4$ *vary from 100% to 40% at engine frequency* $f = 50Hz$.

Keywords: *free-piston linear engine; biogas; computational fluid dynamics; scavenging; simulation.*

Abbreviation:

FPLE	free-piston linear engine	CFD	computational fluid dynamics
LMS	least mean squares	BDC	bottom dead center
HCCI	homogeneous charge compression ignition	UDF	user-define function

1. INTRODUCTION

Within the most potential selection for the conventional engine replacement in terms of hybrid vehicles, FPLE attracts a great number of researchers [1-9]. To study whether the FPLE, which is already known for its high efficiency even reaching 50% indicated efficiency under HCCI operation [5], will be compatible with clean fuels namely biogas or not, it is important to consider the effect of biogas on the engine's performance characteristics itself. When the gas properties vary according to the proportion of biogas components and it directly influence the gas exchange process, which is the key process to improving the engine performance, thus, a scavenging examination is a must to be carried out. CFD is one efficient method to execute the work since it solves the Navier-Stokes equation numerically. Since the cylinder structure uses ports to deliver fresh gas, the scavenging process depends on the fresh gas feeding into the bounce-chamber, hence, the scavenging model and the bounce-chamber gas feeding model should be combined. However, the CFD model is extremely complicated if we include the bounce-chamber geometry. Therefore, simplifying the simulation domain that only maintains the cylinder geometry and calculating the bounce-chamber flow characteristics to define boundary conditions is among the most widely-chosen solutions

(***Figure 1***). There have been an increasing number of reports concerning scavenging simulation using CFD [6-9]. The geometry simulation domains of these studies are only the volume of the cylinder which focus on exchanging fresh gas processes. Nonetheless, boundary conditions computation are ambiguous when it comes to not estimated quantity of fresh gas trapped in the bounce-chamber. In this study, a simple zero-dimensional mathematical model based on the Reynolds transport theorem was built to observe the trapped gas in the bounce-chamber before CFD simulation is implemented. Because the bounce-chamber volume is inconstant as a result of the piston motion, the momentum conservation equation for a deforming control volume is applied.

CFD is a branch of fluid mechanics that uses numerical Navier-Stokes equations to handle the streamline of fluid flow as well as the interaction between it and boundary surfaces. This paper uses the finite volume method, which has advantages in memory usage and calculation speed, especially for solving turbulent flows with high Reynolds number. The $k-\varepsilon$ turbulent model is also applied since the main aim of this work is to measure the trapped fresh gas's mass for thermodynamic simulation in further work, which does not need good predictions in the region near boundaries. Besides, a dynamics mesh is also used in which the piston motion is coded based on the UDF library and compiled by a C++ compiler.

Biogas, which is derived from anaerobic digestion of organic materials primarily contains methane (50-75%), carbon dioxide (25-50%), and may exist insignificant amounts of hydrogen sulfide (0.1-0.5%), moisture and siloxanes. When assuming that biogas has only methane and carbon dioxide, the properties of the fluid which is used in CFD simulation must be in corresponding with the variation of methane percentage. Gas properties that directly affect the CFD simulation are density, viscosity. By applying the least mean squares (LMS) technique, these properties are approximated to multivariable functions from discrete data of every individual mixture's elements. These data were collected from [10]. All of these boundary conditions and gas properties will become an input of CFD modeling afterward.

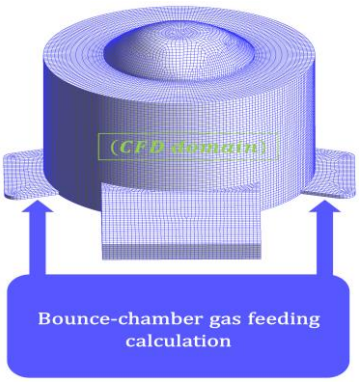

Figure 1. *Simplify the simulation domain.*

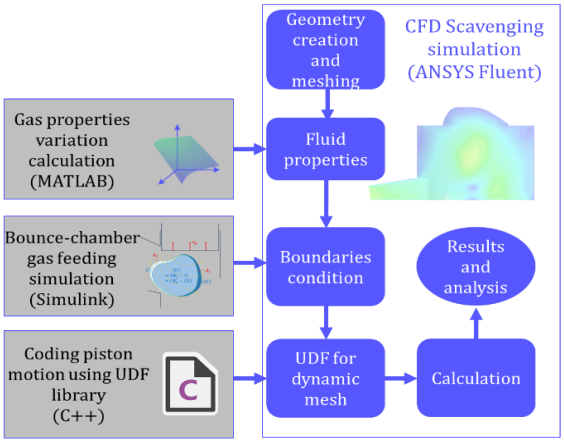

Figure 2. *Illustration of workflow.*

2. MATHEMATICAL MODELLING

2.1 Mixture properties estimate

Density, kinematic viscosity, dynamic viscosity of methane, carbon dioxide, and atmosphere (are collectively referred to as parameter B) are approximated to second-order polynomials with temperature. With the data is discrete $B = \{(T_1, B_1), (T_2, B_2), \dots (T_n, B_n)\}$ fitted to $f(T) = B(T) = \alpha T^2 + \beta T + \gamma$, where T denotes the gas temperature. When the biogas is supposed a mixture of CH_4 and CO_2, the parameter B of biogas is evaluated by:

$$B_{biogas}(T) = \Omega B_{CH_4}(T) + \Psi B_{CO_2}(T) \quad (1)$$

where Ω, Ψ denotes the volumetric percentage of CH_4 and CO_2 component

respectively. The ideal chemical reaction of biogas combustion can be written as:

$$\Omega CH_4 + \Psi CO_2 + 2\Omega\left(O_2 + \frac{79}{21}N_2\right) \xrightarrow{t^0} (\Omega + \Psi)CO_2 + 2\Omega H_2O + \frac{158}{21}\Omega N_2 + Q_{out}$$

According to that, the parameter *B* of the mixture can be determined when the engine is operating at the air-fuel equivalence ratio λ:

$$B_{mix}(T) = \frac{1}{1 + 2\lambda\Omega}\left[B_{biogas}(T) + 2\lambda\Omega B_{atmosphere}(T)\right] \quad (2)$$

2.2 The bounce-chamber gas flow model

The fresh gas must be provided into the bounce-chamber before being pushed by the piston's motion to the combustion chamber via transfer ports. Consequently, the parameters at the end of the bounce-chamber gas feeding process are the boundary conditions for the gas exchange process. The parameter X has the x, which is the amount of *X* per unit mass:

$$X = \iiint x\rho dW \quad (3)$$

where ρ is the gas density, W is the control volume. The time rate of change of X is described below:

$$\frac{DX}{Dt} = \left(\frac{\partial X}{\partial t}\right)_W + \oiint x\rho(\vec{u}\cdot\vec{n})dA \quad (4)$$

where $\vec{n}$ is the unit normal vector, $\left(\frac{\partial X}{\partial t}\right)_W$ is the partial derivative to time of X in the system W while $\oiint x\rho(\vec{u}\cdot\vec{n})dA$ is the net flux of *X* through the control surface A.

With $X = m\vec{u}$ is the flow's linear momentum ($x = \vec{u}$):

$$\frac{D(m\vec{u})}{Dt} = \sum \overrightarrow{F_{external}} = \frac{\partial}{\partial t}\iiint \rho\vec{u}dW + \oiint \rho\vec{u}(\vec{u}\cdot\vec{n})dA \quad (5)$$

Usually, the flow velocity when the engine operating at lower than $5000\ rpm$ is not greater than $100m/s$, which means the Mach number is smaller than 0.3 and, thus, the gas flow is incompressible. Besides, to reduce the complication of the model, the flow streamline is assumed perpendicular to sections $1-1, 2-2$. Since the piston moves at velocity v_p, the control volume is deformed at v_p at the piston bottom surface, hence, relative velocities are used instead. The multiply $(\vec{u}\cdot\vec{n})$ will be equal to $|\vec{u}||\vec{n}|cos\left(\frac{\pi}{2}\right)$ or $|\vec{u}||\vec{n}|cos\left(-\frac{\pi}{2}\right)$ when the flow's streamline is perpendicular to sections and accordingly, it equals either u or $(-u)$ if the gas flow direction is outward or inward the control volume. On the other hand, the velocity profile is nonuniform, the average velocity can be used instead, with the momentum-flux correction factor Γ:

$$\int \rho\vec{u}(\vec{u}\cdot\vec{n})dA = \rho\Gamma\int \bar{u}^2 dA \quad (6)$$

Since the flow is turbulent, leading to Γ varying from 1.01 to 1.04 respectively [11]. These are almost unity that we can normally neglect it ($\Gamma = 1$). The external forces when we ignore the friction between the gas and the wall are the forces due to static pressure at sections. When the piston moves upward:

$$\frac{\partial}{\partial t}\left(\rho\iiint \overline{u_1}W\right) - \rho\iint \overline{u_1}^2 dA_1 = p_1A_1 - \frac{\partial}{\partial t}\left(\rho\iiint \overline{v_p}W\right) \quad (7)$$

When the piston moves downward:

$$\frac{\partial}{\partial t}\left(\rho\iiint \overline{u_1}W\right) - \rho\iint \overline{u_1}^2 dA_1 = p_1A_1 + \frac{\partial}{\partial t}\left(\rho\iiint \overline{v_p}W\right) - \rho\iint \overline{u_2}^2 dS \quad (8)$$

where $u_2 = \frac{A_1}{S}u_1 + v_p$ and all pressures used in this paper are gauge pressure.

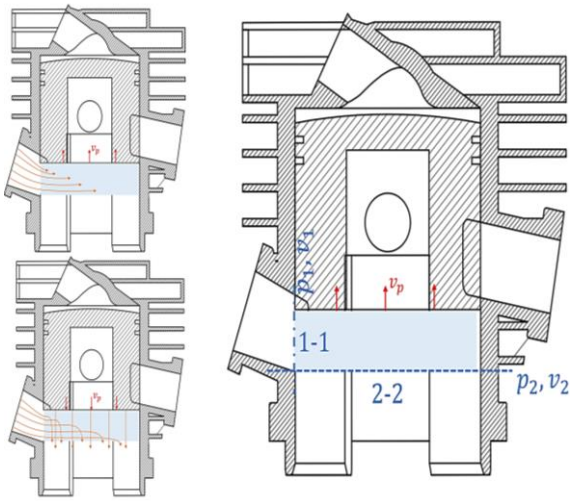

Figure 3. *Cross-section of the cylinder.*

3. SIMULATION

3.1 Boundaries determination

Table 1. *Engine's important parameters.*

Parameters	Unit	Value
Piston diameter	mm	45
Piston displacement	mm	31
Cylinder volume	cm^3	49.3
Piston displacement that intake port is opened	mm	11.7
Piston displacement that transfer ports are opened	mm	6.3
Bounce-chamber volume	cm^3	58.3

The model was built via Simulink, in which the cylinder dimensional parameters are coded in a script file. Important parameters of the modeled engine are listed in the table below. The model calculates separately for piston upward and downward, then the velocity is merged into one signal to integrate with time to obtain the supplied gas quantity. Because the model is segregated, the last value in the piston upward subsystem is driven to initial condition for the piston downward subsystem. The duration of piston downward and upward is controlled by the piston displacement and the sign of the piston velocity. When the piston bottom completely closes the intake port, the simulation is triggered to stop.

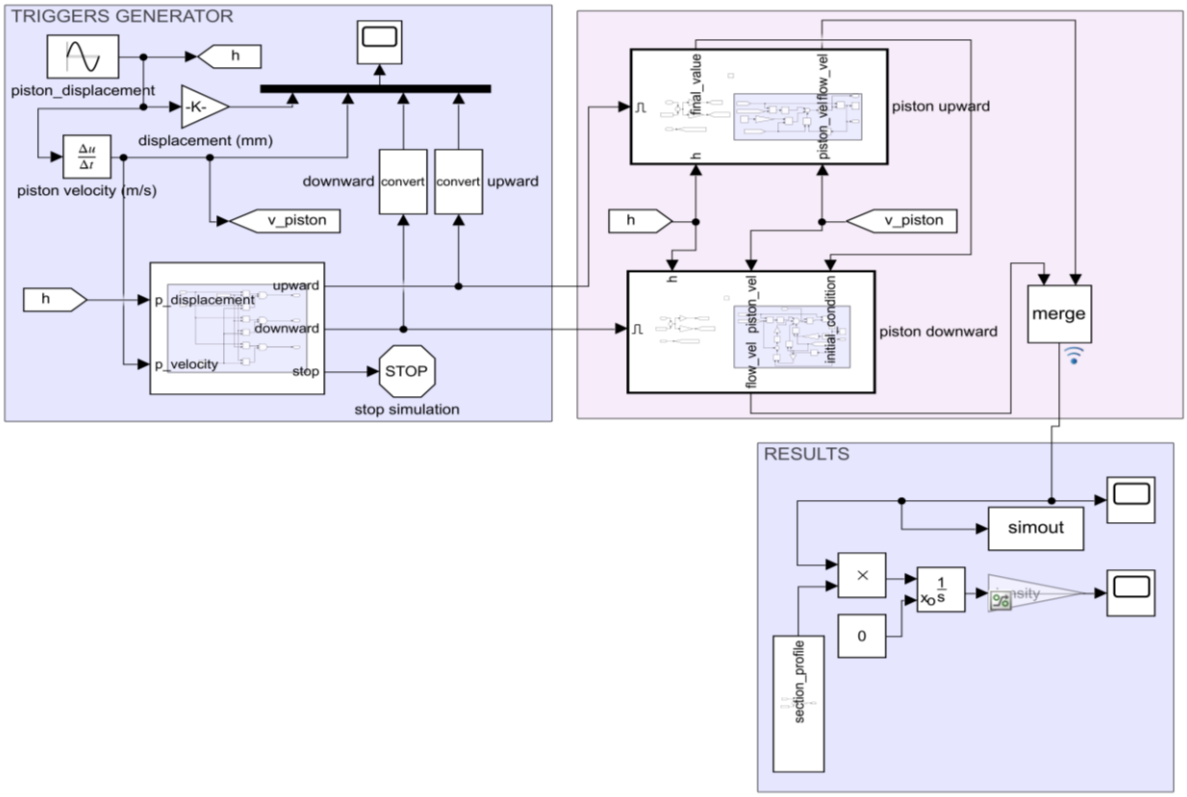

Figure 4. *Modeling for bounce-chamber gas feeding period using Mathworks Simulink.*

3.2 Meshing methodology

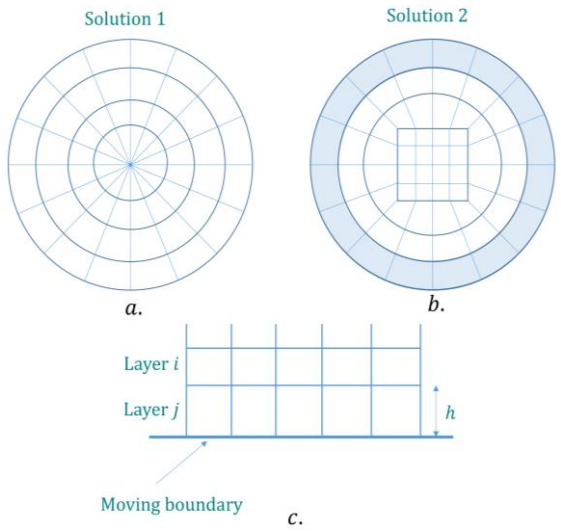

Figure 5. *Solutions for cylinder meshing: a) solution 1. b) solution 2. c) layering method.*

The CFD simulation domain is divided into a large number of cells, which this work is well-known as meshing. With the cylindrical geometry of the combustion chamber, the idea is using hexahedron or prism cells. It arrives at the solution 1 (***Figure 5a***), in which triangular prism cells contact each other at the cylinder's center and are surrounded by tetragonal prism cells. However, the exhaust pipe can not be meshed using prism cells, leading to impossible sharing topology between the cylinder and the exhaust pipe. In solution 2 (***Figure 5b***), a subdomain which contains square prism cells is created, so it allows using both prism cells and hexahedron cells (the blue area) in cylinder geometry. The solution 2 permits connecting the cylinder's mesh and exhaust pipe's mesh since hexahedron cell type is applied in the exhaust pipe.

The piston motion is divided into steps that the mesh updating in every time step is obligated. Since the motion of the piston is perpendicular to the piston top's plane, the layering method is chosen. The layer of cells adjacent to the moving boundary (layer j) is split or merged with the next layer (layer i). If the layer j is expanding, the height of cells in it increases until: $h_{min} > (1 + \alpha_s)h_{ideal}$, where h_{min} is the minimum height of cells in layer j, h_{ideal} is the ideal cell height, and α_s is the split factor. Two new layers are created with their height respectively is h_{ideal} and $(h - h_{ideal})$ or the ratio of their height is equal α_s. On the contrary, if the layer j is being compressed, it can be compressed until: $h_{min} < \alpha_c h_{ideal}$, where α_c is collapse factor. When the condition is met, layer j and i are merged.

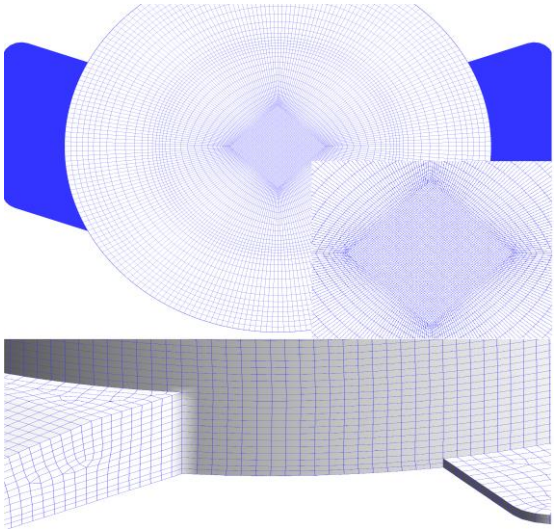

Figure 6. *Applied the solution 2.*

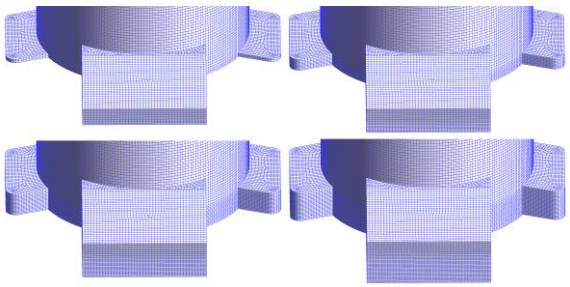

Figure 7. *The mesh updated by using the layering method.*

4. RESULTS AND DISCUSSION

4.1 Gas characteristics

The result in ***Figure 8*** shows that when the $\%CH_4$ increases, although the density of biogas increases, the ideal mixture's density decreases. This is the reason that the more C molecules in biogas, the more oxidative molecules are required. The graph demonstrates the mixture's dynamics viscosity is not affected much by $\%CH_4$ in the region of $20\%CH_4$ to $100\%CH_4$, but by

the temperature. The ideal mixture' characteristics at the atmosphere temperature $30°C$ was collected for 5 circumstances of biogas component: $40\%\ CH_4$, $50\%\ CH_4$, $60\%\ CH_4$, $70\%\ CH_4$, and $100\%\ CH_4$ (***Figure 9***). These values will be saved as the input database for fluid declaration in CFD modeling afterward.

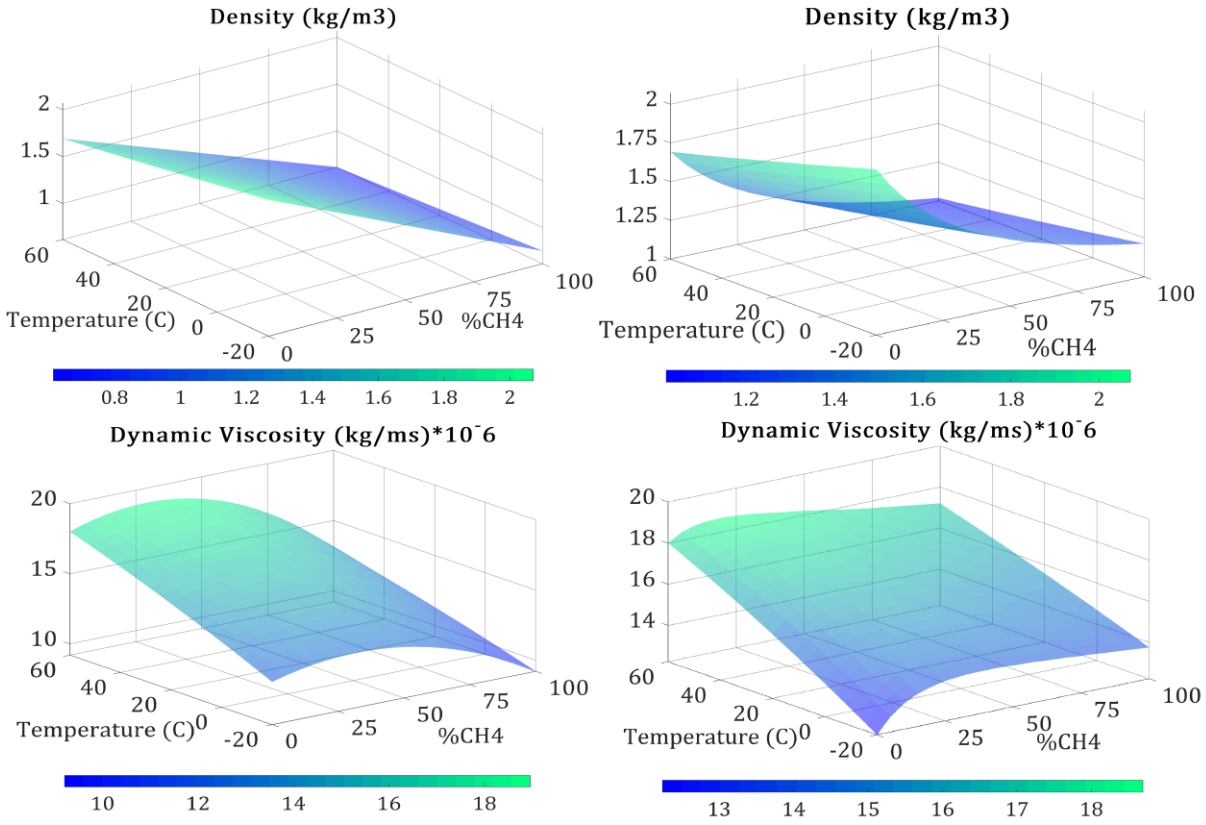

Figure 8. *Density, viscosity (up to down respectively) of biogas (left) and the ideal mixture (right) corresponding to $\%CH_4$ and temperature.*

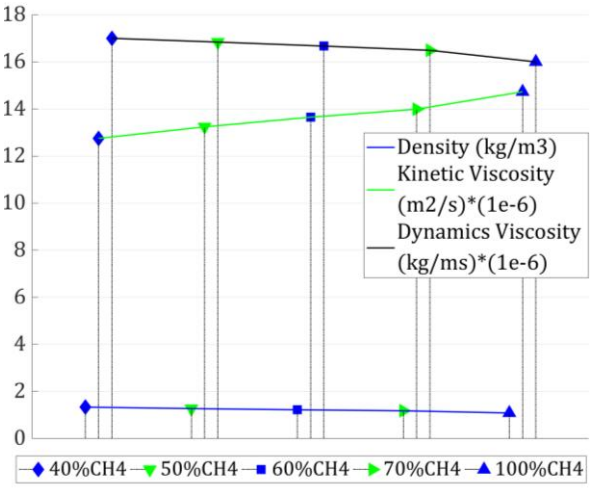

Figure 9. *Density, kinetic viscosity, and dynamic viscosity of ideal mixture variation at $30°C$.*

4.2 Bounce-chamber gas feeding results

The gas flow velocity at the intake port's section is shown in ***Figure 10***, in which the time $0ms$ relates to the piston top at BDC. The velocity shape expresses that the gas was pulled by the piston acceleration during piston moving upward before being pushed by the inertia itself during piston moving downward. The trapped mass of gas in the bounce-chamber is also shown in ***Figure 11***. The result indicates that at the engine's frequency equals $16.67Hz$ (equivalent $1000rpm$ at conventional engine), the delivered gas quantity is exceedingly low (0.0353 gram) bringing the maximum volumetric efficiency can be achieved in

scavenging process at only 0.5395 (when using 40% CH_4 biogas) and therefore, it may be unable to operate the engine. Besides, volumetric efficiency can reach 0.7386 when the engine operates at frequency 83.33Hz (equivalent $5000rpm$).

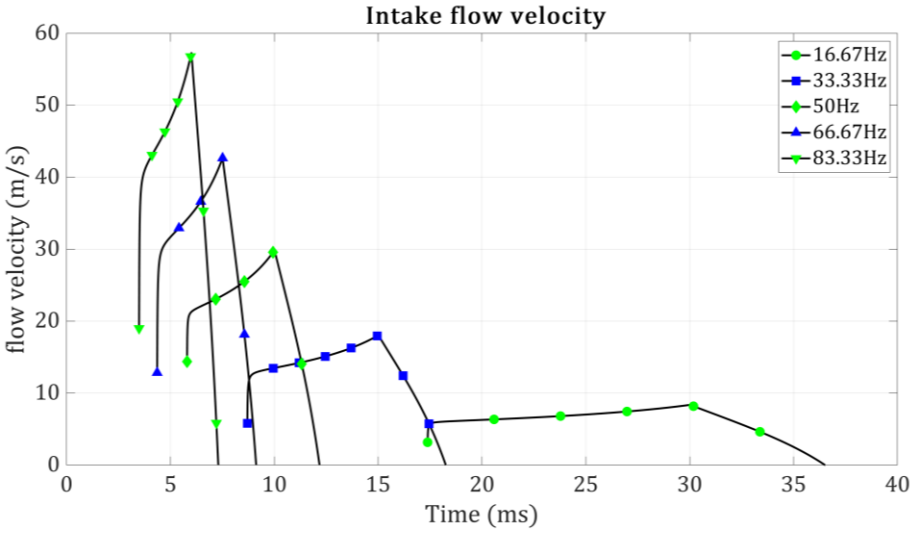

Figure 10. *Flow velocity at the intake port section.*

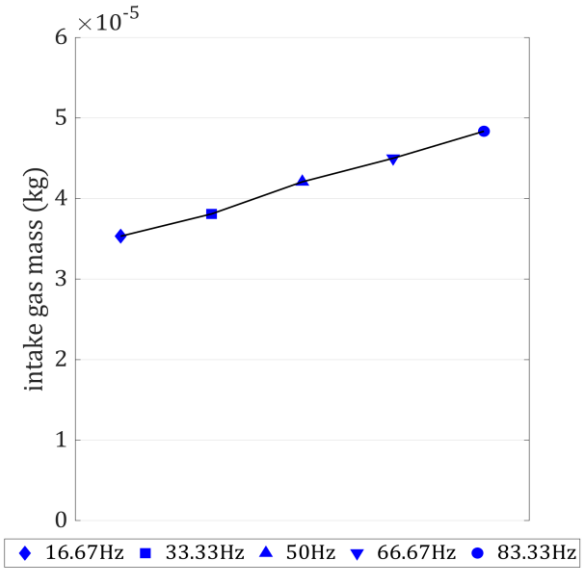

Figure 11. *Quantity of fresh gas into the bounce-chamber.*

4.3 CFD simulation results

The velocity vector field is shown in ***Figure 12***, in which the methane percentage in biogas was set to 40%. A high – speed and great directed tumble comes about in the simulation. The combustion efficiency may be enhanced as a consequence of the tumble closer the TDC during the piston moves upward, which helps the flame propagating speed more rapidly. The turbulent flow, which can be seen in ***Figure 13***, is more strong in higher engine frequency (based on flow's streamlines and flow's velocity). Flow's velocity is highest at the transfer port's cross-section ($\approx 160m/s$ at $f = 16.7Hz$, $\approx 190m/s$ at $f = 33.3Hz$ and $\approx 250m/s$ at $f = 50Hz$) while inside the cylinder, velocity range is significantly lower ($\approx 40 - 90m/s$ at $f = 16.7Hz$, $\approx 60 - 120m/s$ at $f = 33.3Hz$ and $\approx 100 - 190m/s$ at $f = 50Hz$). Besides, the in-cylinder pressure at the end of the intake process, which is a parameter to import to the thermodynamics model in further work, is obtained. Especially, it is more important since FPLE needs to control accurately piston motion to assure stable operation. The higher in-cylinder pressure, the more energy needed for compression. The pressure distribution is shown in ***Figure 14***. When the engine operates at 16.6Hz, the pressure $p_a \approx 1.012\ bar$, and it is higher at engine frequency $f = 33.3Hz$ ($p_a \approx 1.04\ bar$) and engine frequency $f = 50Hz$ ($p_a \approx 1.08\ bar$). The pressure is slightly lower at the center cylinder due to the turbulent phenomenon.

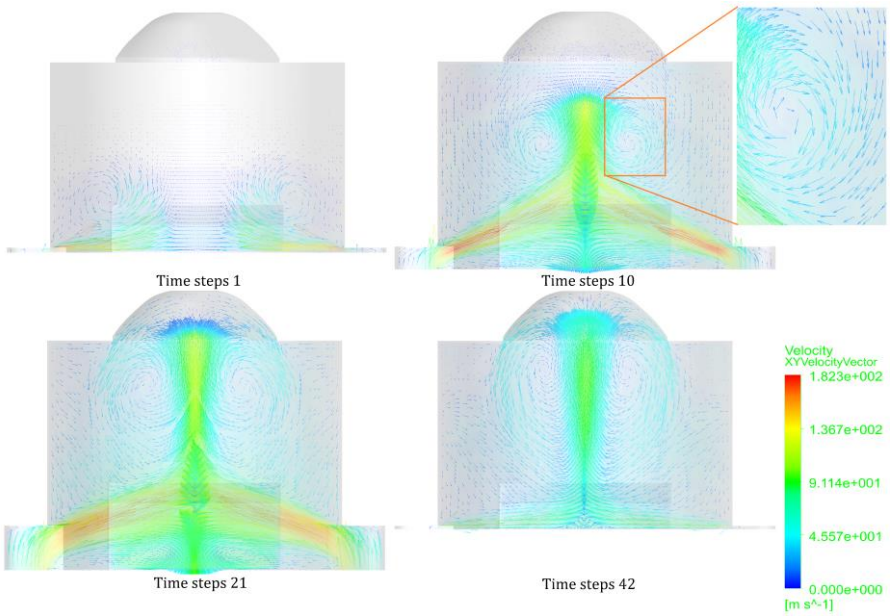

Figure 12. *The velocity vector field at the cylinder cross-section when the engine operates at 16.6Hz fueled with* 40% $CH4$ *biogas.*

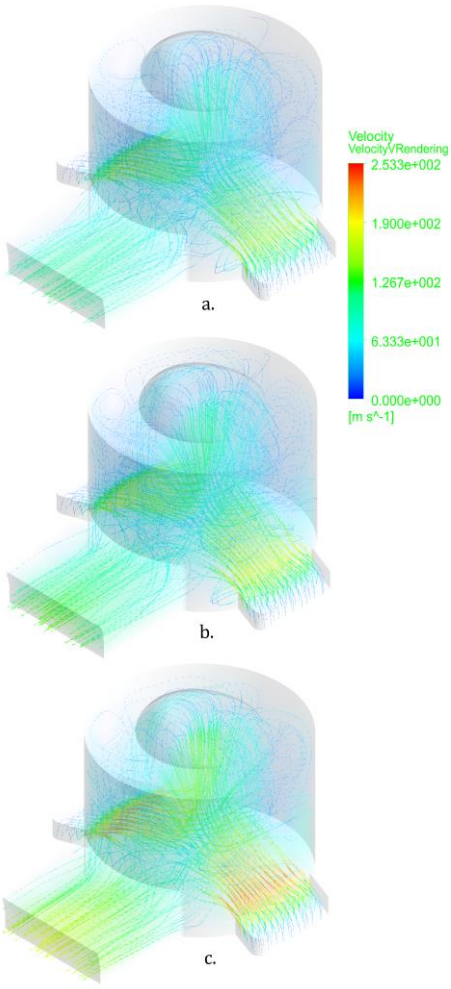

Figure 13. *The velocity streamlines at engine frequency: a. 16.6Hz b. 33.3Hz c. 50Hz.*

Figure 15 shows how the mass flow rate is influenced by time during intake at engine frequency 50Hz. It demonstrates that using biogas which have 40% CH_4 will have the highest mass flow rate. The mass flow rate is rapidly decreasing at the beginning in which the piston top just opens transfer ports, and then grows again. This is due to the open sectional area is still small, and thus, reversed flows can appear as a result of contact between flows and boundaries. ***Figure 16*** shows the delivered gas mass into the cylinder at engine frequency 16.6Hz, 33.3 Hz and 50Hz for 5 circumstances of biogas component proportion 40% CH_4, 50% CH_4, 60% CH_4, 70% CH_4, 100% CH_4. The effect of methane percentage can be easily seen, which the more methane quantity in biogas, the less gas mass delivered into the cylinder. The maximum gas mass is 0.0403 gram when the engine operates at $f = 50Hz$ and fueled with 40% CH_4. However, the intake efficiency is increased following the %CH_4 augmentation (***Figure 17***), particularly from 0.612 to 0.679 when %CH_4 vary from 40% to 100% at engine frequency $f = 50Hz$. This is because of the mixture density decreases when we increase %CH_4.

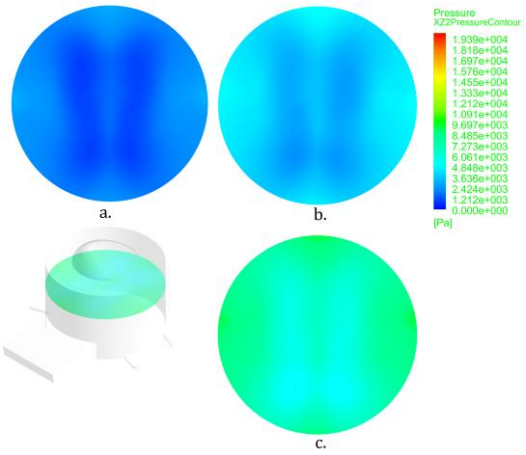

Figure 14. *In-cylinder pressure distribution at the end of scavenging when using 40%CH4 biogas: a. engine operates at 16.6Hz b. engine operates at 33.3Hz c. engine operates at 50Hz.*

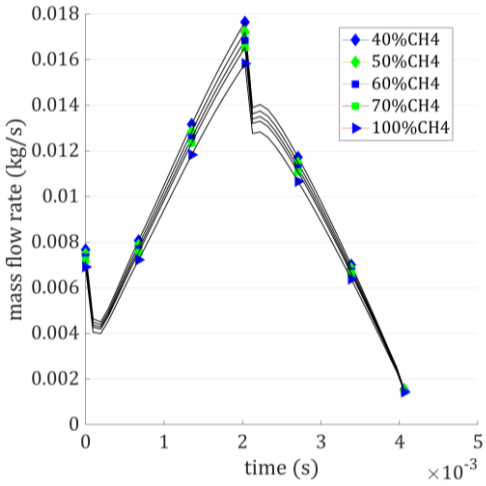

Figure 15. *The mass flow rate at the transfer port's section at engine frequency $f = 50Hz$.*

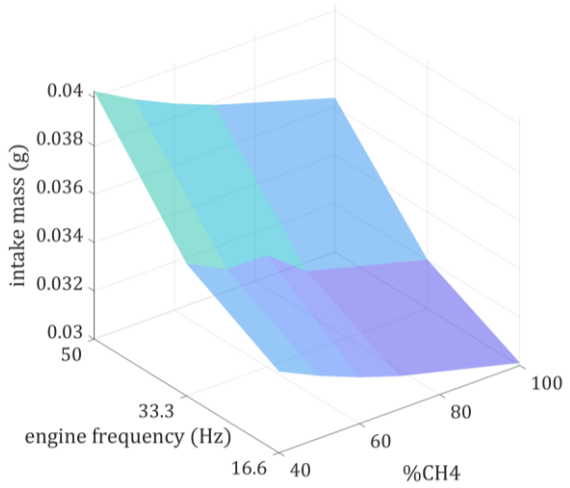

Figure 16. *Delivered gas mass into the cylinder.*

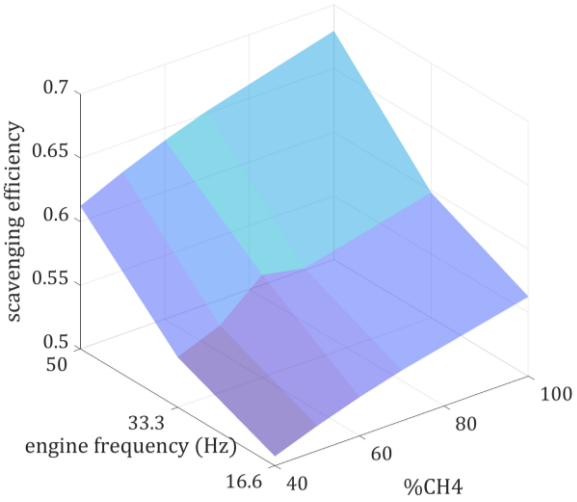

Figure 17. *The map of volumetric efficiency.*

5. CONCLUSION

A CFD scavenging simulation in a two-stroke free-piston linear engine fueled with biogas has been successfully modeled, in which, the boundary conditions are determined based on a zero-dimensional model. Simultaneously, the variation of fresh gas characteristics has been completely observed to be used as the fluid in CFD modeling. The result shows that although delivered gas mass is enhanced when using low $\%CH_4$ biogas, the intake efficiency is decreased, particularly from 0.612 to 0.679 when $\%CH_4$ vary from 40% to 100% at engine frequency $f = 50Hz$.

In the next work, using CFD software to simulate scavenging in FPLE is continued for other lambda circumstances. Then, the thermodynamics model will be built to explore the effect of methane percentage in biogas on the engine power output.

REFERENCES

[1] Boru Jia, Z. Zuo, A. Smallbone, H. Feng, A. P. Roskilly. (2017). A Decouple Design Parameter Analysis for Free Piston Engine Generators. *energies*.

[2] H. Kosaka, T. Akita, K. Moriya, S. Goto, Y. Hotta, T. Umeno, K. Nakakita. (2014). Development of Free Piston Engine Linear Generator System Part 1 - Investigation of Fundamental Characteristics. *SAE Technical Paper*.

[3] H. Kosaka, T. Akita, K. Moriya, S. Goto, Y. Hotta, T. Umeno, K. Nakakita. (2014). Development of Free Piston Engine Generator Part 2 - Investigation of Control System for Generator. *SAE Technical Paper*.

[4] R. Mikalsen, A. P. Roskilly. (2008). The design and simulation of a two-stroke free-piston compression ignition engine for electrical generation. *Applied Thermal Engineering*, 589-600.

[5] P. V. Blarigan, N. Paradiso, S. Goldsborough. (n.d.). Homogeneous Charge Compression Ignition with a Free Piston: A New Approach to Ideal Otto Cycle Performance. *SAE Technical Paper*.

[6] Nguyen Ba Hung, Sung Jaewon, Ocktaeck Lim. (2017). A study of a scavenging process in a two-stroke free piston linear engine using CFD. *9th International Conference on Applied Energy* (pp. 1354-1360). Cardiff, UK: Elsevier Ltd.

[7] S. G. Karunanidhi, Nithin V. S, G. Subba Rao. (2014). CFD studies of two-stroke petrol engine scavenging. *Journal of Engineering Research and Application*, 74-79.

[8] Xuetian Lu, Fujun Zhang, Yuhang Liu, Sufei Wang. (2018). Analysis on Influences of Scavenging Ports Width to Scavenging Process Based on Opposed Piston Two Stroke Diesel Engine. *10th International Conference on Applied Energy* (pp. 5838-5843). Hong Kong: Elsevier Ltd.

[9] Yining Wu, Yang Wang, Xudong Chen, Shuai Guan, Jiancai Wan. (2014). Three dimensional CFD (Computational fluid dynamics) analysis of scavenging process in a two-stroke free-piston engine. *Energy 68*, 168-173.

[10] Retrieved from Engineering Toolbox: www.engineeringtoolbox.com

[11] White, F. M. (2009). Integral Relations for a Control Volume. In *Fluid Mechanics* (p. 165). McGraw-Hill.

Corresponding author:
Ho Van Phuc
University of Technology, Vietnam National University-Ho Chi Minh City
Email: 1870363@hcmut.edu.vn